EJO
ISSN 1120-6721 | ORIGINAL RESEARCH ARTICLE

European Journal of Ophthalmology
2018, Vol. 28(2) 175–181

DOI: 10.5301/ejo.5001033
journals.sagepub.com/home/ejo
SAGE

Morphology of the optic nerve head in glaucomatous eyes with visual field defects in superior or inferior hemifield

Antonio Longo, Teresio Avitabile, Maurizio G. Uva, Vincenza Bonfiglio, Andrea Russo, Mario D. Toro, Salvatore Faro, Michele Reibaldi

Eye Clinic, University of Catania, Catania - Italy

ABSTRACT

Purpose: To evaluate the morphology of optic nerve head (ONH) and border tissue (BT) of Elschnig in glaucomatous eyes with visual field defects in superior or inferior hemifield.
Methods: In a case-control study, we included 25 patients with superior arcuate scotoma, 25 patients with inferior arcuate scotoma, and 25 healthy controls. They received visual field testing, measurement of peripapillary retinal nerve fiber layer (RNFL) thickness, and ONH examination in a radial pattern with spectral-domain optical coherence tomography. In each ONH scan, the length of Bruch membrane opening (BMO) and BT were measured. Pattern deviation of 6 areas of the visual field and RNFL thickness in corresponding sectors was calculated.
Results: Mean BMO length did not differ between groups. Compared with controls, glaucomatous eyes with superior scotoma had a greater BT length in inferior sectors ($p<0.001$), and eyes with inferior scotoma had a greater BT length in superotemporal sectors ($p = 0.006$). In both groups, a significant correlation was found between BT length and pattern deviation and RNFL thickness of corresponding sectors of superior and inferior hemifields.
Conclusions: In patients with arcuate scotoma in one hemifield, the length of the BT correlates with glaucomatous anatomical and functional damage.

Keywords: Glaucoma, Optical coherence tomography, Optic nerve head, Visual field

Introduction

The main feature of glaucoma is damage to retinal ganglion cells, which leads to axon loss and visual field (VF) alterations (1). Many factors are involved in the pathogenesis of glaucomatous damage, including increased intraocular pressure (IOP), age, race, family history, diabetes, and myopia (2). The specific patterns of glaucomatous changes indicate that the optic nerve head (ONH) is the site of axonal damage, although the mechanisms are not known (3).

Spectral-domain optical coherence tomography (SD-OCT) is a technique used to measure retinal nerve fiber layer (RNFL) thickness and to examine the ONH (4). Studies using SD-OCT have found that the optic disc margin, as clinically detected, depends mainly on the 3D architecture of Bruch membrane and the underlying border tissue (BT) of Elschnig (5, 6). The BT of Elschnig is a fibrous tissue that extends from the anterior edge of the sclera to Bruch membrane and separates the choroid from axons of retinal ganglion cells in the anterior portion of the neural canal (7).

In monkeys, 3 BT configurations have been described in relation to the underlying sclera: internally oblique, externally oblique, and vertical or nonoblique (5, 6). In humans, Reis et al (8) found that BT obliqueness differs between locations in the optic disc and can have 2 or 3 configurations in the same eye. In healthy subjects, the most common configuration is the internally oblique configuration. Glaucomatous eyes with focal damage have an internally oblique configuration in superior and nasal quadrants, and an externally oblique configuration in inferior and temporal quadrants. Patients with diffuse damage have a similar pattern of internally oblique configuration and nearly complete absence of the externally oblique configuration. Patients with sclerotic damage have an internally oblique configuration around the optic disc except inferiorly (8).

Although these characteristics of the optic disc margin have been elucidated, it is unknown whether such configurations are related to glaucomatous damage. The aim of this study was to use SD-OCT to investigate the morphology of the ONH, BT configuration, and peripapillary RNFL thickness

Accepted: August 22, 2017
Published online: September 25, 2017

Corresponding author:
Antonio Longo
Eye Clinic
University of Catania
Via Santa Sofia 78
95123 Catania Italy
ant-longo@libero.it

in patients with glaucomatous VF damage in a superior or inferior hemifield.

Methods

This case-control study included patients with open-angle glaucoma with arcuate scotoma in one hemifield (superior or inferior) and with the other hemifield undamaged. The subjects were recruited at the Glaucoma Center of the Eye Clinic of the University of Catania. A group of healthy subjects who were relatives of hospital staff and nurses served as the control group. The study was performed according to the tenets of the Declaration of Helsinki and was approved by our institutional review board; all subjects gave their informed consent.

The inclusion criteria were a diagnosis of open-angle glaucoma, including primary, pseudoexfoliative, or pigmentary glaucoma; the presence of an arcuate scotoma (in one [superior or inferior] hemifield, with undamaged other hemifield, detected by standard automated perimetry); and focal optic disc damage (superior or inferior notch) detected by slit-lamp observation with +60 D lens. All the patients had a history of high IOP (>24 mm Hg) and had an IOP <18 mm Hg after topical therapy. At the examination, all had best-corrected visual acuity >0.8 Snellen units, refraction within 3.00 D sphere, and 1.00 D astigmatism.

The exclusion criteria were any concomitant ocular disease, previous ocular trauma or surgery, normal-tension glaucoma, any retinopathy, any optic nerve or neurologic disease, or diabetes. Eyes with an ONH with sclerotic or diffuse damage were also excluded. If both eyes were eligible, one eye was randomly selected as the study eye.

In patients fulfilling inclusion and exclusion criteria, VF and SD-OCT examinations were performed on the same day, each by a physician unaware of the aim of the study.

Visual field testing

The VF was tested using the Swedish Interactive Thresholding Algorithm program 24-2 of the Humphrey Field Analyzer (Carl Zeiss Meditec).

All glaucomatous patients had an arcuate scotoma in one (superior or inferior) hemifield, undamaged other hemifield, and focal optic disc damage (superior or inferior notch). Arcuate scotoma and undamaged hemifield were defined according to the Keltner et al (9) classification, which describes an arcuate scotoma as a significant VF loss in the nerve fiber bundle region that extends across contiguous abnormal points from the blind spot to at least 1 point outside 15° adjacent to the nasal meridian. Control subjects had an IOP <18 mm Hg and mean deviation, pattern standard deviation, and glaucoma hemifield test results within normal limits. All patients were well-trained in having their VF tested and had undergone affordable VF testing at least 3 times in the preceding 12 months. A reliable VF had a rate of fixation loss and false-positive and false-negative errors <10%.

Each VF was divided into 6 sectors based on the RNFL-VF scheme described by Garway-Heath et al (10, 11) (Fig. 1). In each sector, the mean pattern deviation was calculated manually using the values of the points of the map by one investigator (M.D.T.) (12). In the temporal sector (sector 6), 2 hemisectors, superior (6A) and inferior (6B), were included. According to Hood and Kardon (13), the decibel level in each VF location was converted to a linear scale (e.g., 0 dB converted to 1.0, 30 dB to 1,000, and - 30 dB to 0.001) before the data were averaged within each sector; the mean value was then converted back to decibel units.

Retinal nerve fiber layer thickness

Peripapillary RNFL thickness was measured using a Spectralis SD-OCT (Heidelberg Engineering GmbH; software Heidelberg Eye Explorer 1.9.10.0) and a circular scan pattern. The scan circle was 12 degrees in diameter, which equated to a retinal diameter of 3.5 mm when assuming a standard corneal curvature of 7.7. All measurements were performed in mydriasis. An internal fixation target was used. Scans with a quality value <15 were excluded (as suggested by the manufacturer), as were those with obvious artefacts such as decentration, incomplete measurement, or blinks. Excluded scans were repeated until good quality was achieved. If the quality of the scans was low after 3 attempts, the patient had to be excluded from the study.

The RNFL thickness values detected in the 6 areas of the Garway-Heath map were included in the analysis. The area under the RNFL thickness curve was measured and was divided by the angular distance (degrees) of each sector using Image J software (version 1.40; available at rsb.info.nih.gov/ij/index.html). In the temporal sector, 6A was the area at 310-354 degrees and 6B was the area at 355-340 degrees on the Garway-Heath map (Fig. 1).

Optic nerve

The ONH was examined using the Spectralis SD-OCT, and a radially equidistant scanning pattern centered on the optic disc included 12 high-resolution 15-degree radial scans, each averaged from 30 B-scans, with 768 A-scans per B-scan. The scanning speed was 40,000 A-scans per second (Fig. 1).

In each OCT scan, the operator first identified the inner margins of the hyperreflective line of Bruch membrane and measured the length of the Bruch membrane opening (BMO). Then he assessed the BT configuration, classified as internally oblique, externally oblique, vertical, or nonoblique according to Reis et al (8) (Fig. 2). Finally, in scans with an externally oblique BT configuration, he measured the length of the BT visualized within the BMO.

For this latter measurement, a line was placed perpendicular to the BMO at the margin of Bruch membrane, and the distance of the most prominent point of the BT protruding into the neural canal from this line was measured (Fig. 3).

For each OCT scan, the 3 assessments (BMO length, BT configuration, BT length) were repeated by 3 independent observers, and the mean value was used in the analyses.

Since each of the sector of the Garway-Heath map was investigated by more than one OCT scan, for correlation with visual field and RNFL thickness, we used the mean of the BT values detected in these scans (Fig. 1).

For the analyses, all values (visual field, RNFL thickness, ONH parameters) are reported for the right eye (temporal at 9 clock hours, nasal at 3 clock hours).

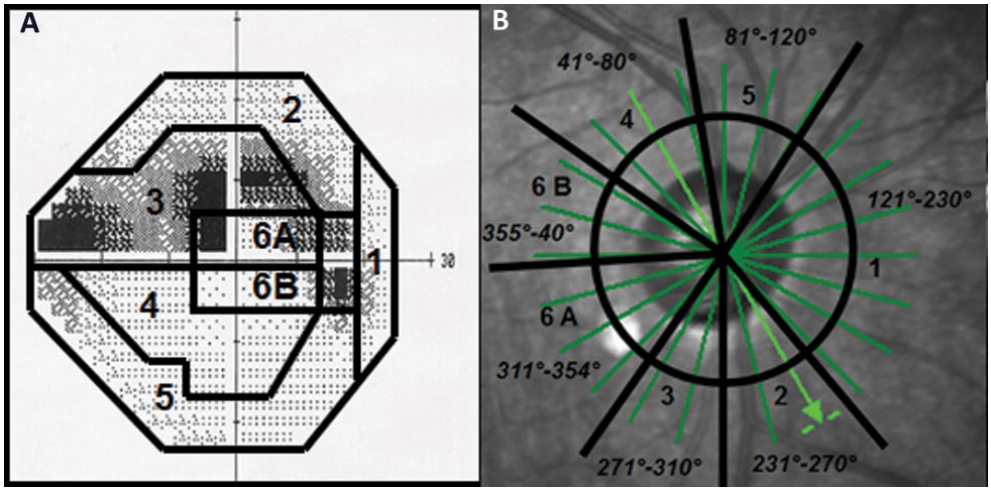

Fig. 1 - Visual field (**A**), retinal nerve fiber layer, and optic nerve head (**B**) regions.

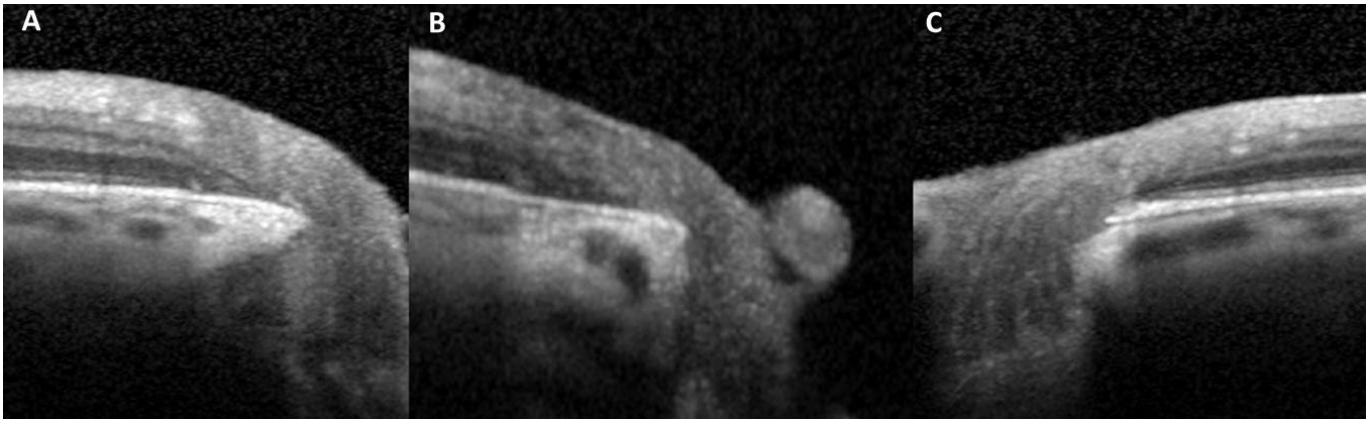

Fig. 2 - Configurations of border tissue: internally oblique (**A**), vertical or nonoblique (**B**), and externally oblique (**C**).

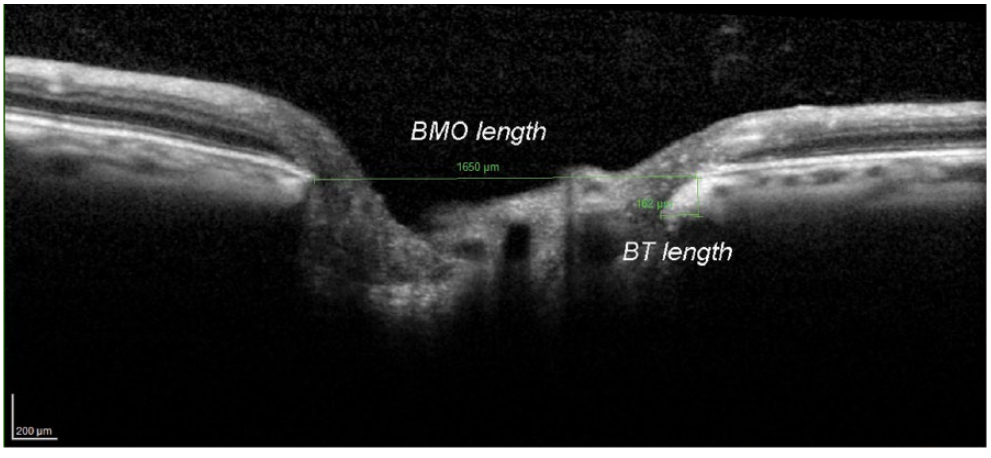

Fig. 3 - Measurement of length of Bruch membrane opening (BMO) and of border tissue (BT) in regions with externally oblique configuration.

Statistical analysis

Analysis of variance (ANOVA) was used to compare the values for the pattern deviation, RNFL thickness, and optic disc parameters between the 2 groups of glaucomatous patients and controls; if significant, Tukey honestly significant difference test was used for multiple comparisons. Pearson correla tion was used to identify correlations between BT length and pattern deviation and RNFL thickness. The coefficients of variation (standard deviation/mean / 100) for BMO and BT length measurements performed by the 3 observers were calculated. SPSS software was used for the analyses (SPSS Inc.).

Results

The subjects were 25 glaucomatous patients with an arcuate scotoma in the superior hemifield, 25 glaucomatous patients with an arcuate scotoma in the inferior hemifield, and 25 healthy controls (Tab. I). No patient was excluded because of low quality of OCT scans.

The mean values for the pattern deviation in different sectors detected in the 3 groups are listed in Table II.

Compared with control eyes, the glaucomatous eyes in both groups had a lower overall RNFL thickness (Tab. III). The mean values were 92 ± 4 µm in controls, 59 ± 5 µm in patients with superior scotoma, and 64 ± 15 µm in patients with inferior scotoma (both comparisons p<0.001). Compared with controls, the RNFL thickness was significantly lower in sectors corresponding to the areas with VF damage: sectors 2, 3, and 6A of eyes with superior scotoma, and sectors 4, 5, and 6B of eyes with inferior scotoma (all p<0.001). The RNFL thickness was also significantly lower in some areas corresponding to undamaged VF: sectors 4 and 6B in eyes with superior scotoma, and sectors 3 and 6A in eyes with inferior scotoma.

Spectral-domain OCT examination showed that, at all hour clock positions, the mean BMO length did not differ significantly among the 3 groups (ANOVA) (Tab. IV).

Table V reports the BT configuration detected at the different radial scans in the 3 groups.

Most of the eyes with superior scotoma had an externally oblique BT configuration in the inferior sectors (21/25, 84%, at the 6 and 7 o'clock positions), and many of those with inferior scotoma had an externally oblique BT configuration in the superior sectors (19/25, 76%, at the 10 and 11 o'clock positions).

Table VI reports the BT length detected at the different radial scans in the 3 groups.

Compared with controls, glaucomatous eyes with superior scotoma had greater BT length in inferior sectors (sectors 2 and 3, scans from 5 to 7 o'clock position, mean BT length 104-126 µm, p<0.001) (Fig. 4), with a correlation between BT length and glaucomatous damage: eyes with higher BT length had lower RNFL thickness (sector 2, r=-0.532, p = 0.006; sector 3, r=-0.613, p<0.001) and higher pattern deviation (sector 2, r=-0.427, p = 0.033; sector 3, r=-0.509, p = 0.009).

TABLE I - Demographics and clinical characteristics of glaucomatous patients and controls

	Superior scotoma (n = 25)	Inferior scotoma (n = 25)	Controls (n = 25)
Age, y	58 ± 7	55 ± 9	54 ± 4
Sex, M/F	12/13	14/11	11/14
Spherical equivalent, D	-0.4 ± 0.5	0.2 ± 0.8	-0.4 ± 1.2
IOP, mm Hg	15.1 ± 1.6	14.8 ± 1.5	13.9 ± 1.3
Mean deviation, dB	-10.5 ± 2.1[a]	-9.1 ± 1.9[a]	-1.5 ± 0.2
Pattern standard deviation, dB	8.7 ± 1.9[a]	8.1 ± 1.7[a]	1.1 ± 0.1

[a]Tukey honestly significant difference vs controls: p<0.001.
IOP = intraocular pressure.

TABLE II - Pattern deviation (decibel, mean ± SD) detected in several sectors of visual field in glaucomatous and control groups

	VF sectors	Superior scotoma (n = 25)	Inferior scotoma (n = 25)	Controls (n = 25)
Superior hemifield	1	-2.0 ± 1.9	-1.0 ± 1.4	-1.2 ± 0.7
	2	-8.1 ± 4.2[a]	-0.9 ± 1.1	-0.6 ± 0.5
	3	-15.7 ± 6.7[a]	-2.3 ± 1.2	-1.2 ± 0.2
	6 A	-11.1 ± 7.6[a]	-1.1 ± 1.7	-0.8 ± 0.8
Inferior hemifield	4	-0.6 ± 1.5	-10.7 ± 3.6[a]	-1.4 ± 0.5
	5	-1.7 ± 2.3	-6.2 ± 2[a]	-1.8 ± 0.8
	6 B	-1.3 ± 0.9	-5.9 ± 3.5[a]	-0.6 ± 0.8

[a]Tukey honestly significant difference vs controls: p<0.001.
VF = visual field.

TABLE III - Peripapillary retinal nerve fiber layer thickness (µm, mean ± SD) detected by spectral-domain optical coherence tomography in several sectors in glaucomatous and control groups

		Superior scotoma (n = 25)	Inferior scotoma (n = 25)	Controls (n = 25)
Overall		59 ± 5[a]	64 ± 15[a]	92 ± 4
Nasal	1	56 ± 11	63 ± 12	63 ± 9
Superior	2	60 ± 14[a]	77 ± 26	104 ± 22
hemifield	3	51 ± 12[a]	87 ± 28[a]	133 ± 14
	6A	45 ± 8[b]	53 ± 11[b]	66 ± 7
Inferior	4	86 ± 11[c]	67 ± 17[a]	139 ± 9
hemifield	5	70 ± 11	60 ± 14[b]	93 ± 15
	6B	56 ± 5[b]	40 ± 9[b]	75 ± 7

[a]Tukey honestly significant difference vs controls: <0.001.
[b]Tukey honestly significant difference vs controls: 0.001.
[c]Tukey honestly significant difference vs controls: 0.026.

TABLE IV - Length of Bruch membrane opening (µm, mean ± SD) as detected by spectral-domain optical coherence tomography (SD-OCT) in different scans in glaucomatous and control groups

SD-OCT scan	Superior scotoma (n = 25)	Inferior scotoma (n = 25)	Control group (n = 25)
12-6 (Superior-inferior)	1,645 ± 109	1,619 ± 72	1,655 ± 125
1-7	1,622 ± 148	1,592 ± 80	1,625 ± 150
2-8	1,547 ± 175	1,572 ± 99	1,575 ± 191
3-9 (Nasal-temporal)	1,542 ± 165	1,540 ± 99	1,567 ± 236
4-10	1,534 ± 157	1,494 ± 85	1,544 ± 232
5-11	1,570 ± 150	1,551 ± 81	1,619 ± 175

Analysis of variance: not significant in all scans.

TABLE V - Border tissue configuration detected in different optic nerve head positions in glaucomatous eyes with superior and inferior scotoma and control groups

	Superior scotoma (n = 25)			Inferior scotoma (n = 25)			Controls (n = 25)		
	IO	NO	EO	IO	NO	EO	IO	NO	EO
12	12	12	1	9	10	6	12	9	4
1	12	13	-	11	13	1	13	8	4
2	10	12	3	13	12	-	14	9	2
3 Nasal	8	13	4	16	9	-	15	9	1
4	7	9	9	12	9	4	15	9	1
5	2	6	17	12	9	4	16	5	4
6	-	4	21	8	12	5	12	7	6
7	-	4	21	5	12	8	10	8	7
8	5	5	15	5	9	11	8	10	7
9 Temporal	7	8	10	2	9	14	8	9	8
10	9	10	6	-	6	19	9	8	8
11	12	12	1	-	6	19	9	7	9

EO = externally oblique; IO = internally oblique; NO = nonoblique.

TABLE VI - Border tissue length (µm, mean ± SD) as detected in different optic nerve head (ONH) positions in glaucomatous and control groups

ONH position	Superior scotoma (n = 25)	Inferior scotoma (n = 25)	Controls (n = 25)
12	3 ± 12	25 ± 46	4 ± 7
1	0	5 ± 24	7 ± 17
2	3 ± 8	0	9 ± 10
3 Nasal	5 ± 12	7 ± 29	4 ± 18
4	25 ± 35	21 ± 48	5 ± 23
5	104 ± 92[a]	22 ± 51	21 ± 48
6	126 ± 63[a]	25 ± 34	25 ± 46
7	109 ± 70[a]	36 ± 49	32 ± 51
8	59 ± 71	61 ± 66	31 ± 50
9 Temporal	51 ± 62	82 ± 7[b]	32 ± 47
10	21 ± 30	109 ± 74[a]	28 ± 41
11	4 ± 20	92 ± 62[a]	32 ± 39

[a] Tukey honestly significant difference vs controls: <0.001.
[b] Tukey honestly significant difference vs controls: 0.016.

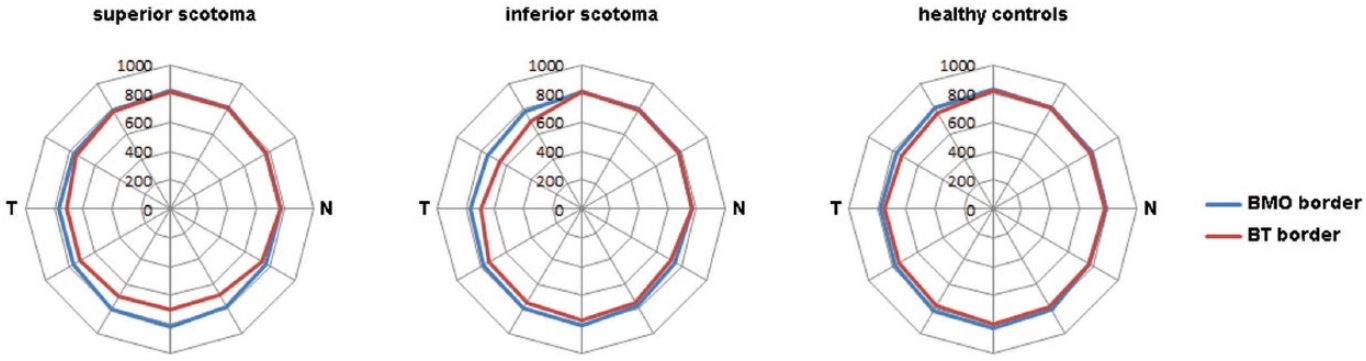

Fig. 4 - Mean length of Bruch membrane opening (BMO) and border tissue (BT) by clock hours.

Glaucomatous eyes with inferior scotoma had a greater BT length in the 9 to 11 o'clock position (sectors 4 and 5, mean BT length 82-109 µm, p = 0.006), with a correlation between BT length and glaucomatous damage: eyes with higher BT length had lower RNFL thickness (sector 4, r=-0.506, p = 0.010; sector 5, r=-0.433, p = 0.031) and higher pattern deviation (sector 4, r=-0.487, p = 0.014; sector 5, r=-0.442, p = 0.027).

The measurement of BMO length and BT length was highly reproducible (coefficients of variation 0.85 and 0.91, respectively).

Discussion

In this study, glaucomatous eyes with VF damage in one hemifield (superior or inferior) had an externally oblique BT configuration in the corresponding area of the ONH, and the BT length was related to the extent of glaucomatous damage (RNFL thickness reduction, pattern deviation).

Using SD-OCT to examine glaucomatous eyes with focal damage, Reis et al (8) found an externally oblique BT configuration in the inferior and temporal quadrants of the ONH and a predominantly internally oblique configuration in the superior and nasal quadrants. The externally oblique configuration was not detected in patients with diffuse damage and was found at the 6 and 7 o'clock positions in 50% of eyes with sclerotic damage.

The oblique configurations of the BT (internal and external) can be found at the 2 sides of the tilted discs and indicate the direction of the tilting, which is related to glaucomatous damage. In a group of myopic patients with normal tension glaucoma, Park et al (14) found 18.45 degrees of inferior torsion of the ONH (inferotemporal tilting) in the presence of a superior VF defect and 3.81 degrees of superior torsion of the ONH (superotemporal tilting) in the presence of an inferior VF defect. They hypothesized that torsion might determine the amount of stress on the optic fibers. In glaucomatous patients,

Choi et al (15) found that the vertical disc tilt relates to the site of damage. In their patients, vertical disc tilt differed between those with a superior and those with an inferior hemifield defect. This observation suggested that there were differences in the susceptibility to glaucomatous damage between the 2 regions.

The termination of the BT of Elschnig constitutes the temporal disc margin in most eyes with β-zone peripapillary atrophy (16). A wide area of β-zone atrophy is associated with glaucomatous alterations and varies according to the location of the VF defect (17). Teng et al (18) showed that the region with the largest β-zone atrophy area predicts the location with the most rapid progression of VF defects. All of these findings suggest that the morphology of the peripapillary area is related to glaucomatous damage.

Previous studies have found a correlation between the sensitivity or pattern deviation of sectors of the VF and RNFL thickness (19, 20), rim area (11, 18), or both (21), and between the localized rim area and RNFL thickness (20). For values measured using the Spectralis SD-OCT, a high correlation has been reported between RNFL thickness and new parameters of the rim, such as the mean minimum rim width and minimum rim area (22), and BMO − minimum rim width (23). These parameters are related to the thickness of the rim in different regions of the optic disc.

We evaluated the relationship between the glaucomatous damage and the structures around the optic nerve. We found that BT morphology is related to glaucomatous damage and suggests that some specific configurations may indicate a greater susceptibility to localized glaucomatous damage, as has been hypothesized (14, 15). Glaucomatous damage has some typical features. Although high IOP affects all retinal ganglion cells and axons, the damage is often localized to specific axon bundles, and the morphology of the defect indicates that the damage occurs at the ONH. Several factors contribute to the damage, including localized circulatory alterations, susceptibility of the lamina cribrosa to IOP, and myopic changes in the papillary area.

The BT configuration may be an additional factor. Our results suggest that in these areas, there is localized damage; in presence of increased IOP, axons could be pressed against the fibrous border tissue, leading to localized blood flow impairment or reduction in the axoplasmic flow. However, we found that glaucomatous eyes also have a reduction in RNFL thickness in sectors corresponding to the unaffected hemifield, as previously reported (24, 25).

This work has several limitations. First, we included patients with specific alterations in the VF and with a typical ONH alteration (notching). Further studies should assess the relationship between VF defects and other papillary morphologies. Second, this study included subjects with a specific range of refraction; the relationship in highly myopic or hyperopic patients should be evaluated. Third, BMO and BT length were measured manually. In high-quality SD-OCT scans, the borders of BM are easily recognizable. In our study, the measurement of both parameters was highly reproducible, as shown by the low coefficients of variation (<1%). However, improved software to provide automatic positioning of the markers and measurements should be useful.

In conclusion, we found that eyes with glaucomatous damage localized in one hemifield had an externally oblique BT configuration in opposite ONH sectors, and that BT length correlated with both RNFL thickness and VF alterations.

Disclosures

Financial support: No financial support was received for this submission.
Conflict of interest: None of the authors has conflict of interest with this submission.

References

1. Quigley HA. Glaucoma. Lancet. 2011;377(9774):1367-1377.
2. European Glaucoma society Terminology and guidelines for glaucoma. 3rd edition, Dogma Publ, Savona, Italy, 2008.
3. Nickells RW, Howell GR, Soto I, John SW. Under pressure: cellular and molecular responses during glaucoma, a common neurodegeneration with axonopathy. Annu Rev Neurosci. 2012;35:153-179.
4. Sung KR, Kim JS, Wollstein G, Folio L, Kook MS, Schuman JS. Imaging of the retinal nerve fibre layer with spectral domain optical coherence tomography for glaucoma diagnosis. Br J Ophthalmol. 2011;95(7):909-914.
5. Strouthidis NG, Yang H, Reynaud JF, et al. Comparison of clinical and spectral domain optical coherence tomography optic disc margin anatomy. Invest Ophthalmol Vis Sci. 2009;50(10): 4709-4718.
6. Strouthidis NG, Yang H, Downs JC, Burgoyne CF. Comparison of clinical and three-dimensional histomorphometric optic disc margin anatomy. Invest Ophthalmol Vis Sci. 2009;50(5): 2165-2174.
7. Nevarez J, Rockwood EJ, Anderson DR. The configuration of peripapillary tissue in unilateral glaucoma. Arch Ophthalmol. 1988;106(7):901-903.
8. Reis AS, Sharpe GP, Yang H, Nicolela MT, Burgoyne CF, Chauhan BC. Optic disc margin anatomy in patients with glaucoma and normal controls with spectral domain optical coherence tomography. Ophthalmology. 2012;119(4):738-747.
9. Keltner JL, Johnson CA, Cello KE, et al. Ocular Hypertension Treatment Study Group. Classification of visual field abnormalities in the ocular hypertension treatment study. Arch Ophthalmol. 2003;121(5):643-650.
10. Garway-Heath DF, Poinoosawmy D, Fitzke FW, Hitchings RA. Mapping the visual field to the optic disc in normal tension glaucoma eyes. Ophthalmology. 2000;107(10):1809-1815.
11. Garway-Heath DF, Holder GE, Fitzke FW, Hitchings RA. Relationship between electrophysiological, psychophysical, and anatomical measurements in glaucoma. Invest Ophthalmol Vis Sci. 2002;43(7):2213-2220.
12. Danesh-Meyer HV, Carroll SC, Ku JY, et al. Correlation of retinal nerve fiber layer measured by scanning laser polarimeter to visual field in ischemic optic neuropathy. Arch Ophthalmol. 2006;124(12):1720-1726.
13. Hood DC, Kardon RH. A framework for comparing structural and functional measures of glaucomatous damage. Prog Retin Eye Res. 2007;26(6):688-710.
14. Park HY, Lee K, Park CK. Optic disc torsion direction predicts the location of glaucomatous damage in normal-tension glaucoma patients with myopia. Ophthalmology. 2012;119(9): 1844-1851.
15. Choi JA, Park HY, Shin HY, Park CK. Optic disc tilt direction determines the location of initial glaucomatous damage. Invest Ophthalmol Vis Sci. 2014;55(8):4991-4998.

16. Park SC, De Moraes CG, Tello C, Liebmann JM, Ritch R. In-vivo microstructural anatomy of beta-zone parapapillary atrophy in glaucoma. Invest Ophthalmol Vis Sci. 2010;51(12):6408-6413.
17. Park KH, Tomita G, Liou SY, Kitazawa Y. Correlation between peripapillary atrophy and optic nerve damage in normal-tension glaucoma. Ophthalmology. 1996;103(11):1899-1906.
18. Teng CC, De Moraes CG, Prata TS, et al. The region of largest β-zone parapapillary atrophy area predicts the location of most rapid visual field progression. Ophthalmology. 2011;118(12):2409-2413.
19. El Beltagi TA, Bowd C, Boden C, et al. Retinal nerve fiber layer thickness measured with optical coherence tomography is related to visual function in glaucomatous eyes. Ophthalmology. 2003;110(11):2185-2191.
20. Aptel F, Sayous R, Fortoul V, Beccat S, Denis P. Structure-function relationships using spectral-domain optical coherence tomography: comparison with scanning laser polarimetry. Am J Ophthalmol. 2010;150(6):825-833.
21. Nilforushan N, Nassiri N, Moghimi S, et al. Structure-function relationships between spectral-domain OCT and standard achromatic perimetry. Invest Ophthalmol Vis Sci. 2012;53(6): 2740-2748.
22. Gardiner SK, Ren R, Yang H, Fortune B, Burgoyne CF, Demirel S. A method to estimate the amount of neuroretinal rim tissue in glaucoma: comparison with current methods for measuring rim area. Am J Ophthalmol. 2014;157(3):540-9. e1, 2.
23. Pollet-Villard F, Chiquet C, Romanet JP, Noel C, Aptel F. Structure-function relationships with spectral-domain optical coherence tomography retinal nerve fiber layer and optic nerve head measurements. Invest Ophthalmol Vis Sci. 2014;55(5):2953-2962.
24. Hoffmann EM, Medeiros FA, Sample PA, et al. Relationship between patterns of visual field loss and retinal nerve fiber layer thickness measurements. Am J Ophthalmol. 2006;141(3): 463-471.
25. Grewal DS, Sehi M, Greenfield DS. Diffuse glaucomatous structural and functional damage in the hemifield without significant pattern loss. Arch Ophthalmol. 2009;127(11):1442-1448.